

# Roll, Ride, Stride: The Ultimate School Commute Showdown

## Technical Report

Group F: Fred Feng, Oliver Meek, Jinze Zhu, Judi Ashri, David Guo, Yuchao Niu, Natalie Minda

## Background

Clean air is vital to life, and when the air is polluted with harmful gaseous air pollutants it negatively affects all living things who rely on clean air for life and for good health. The surrounding air that we breathe can be contaminated through the emission of gaseous substances into the atmosphere such as nitrogen oxides (NO<sub>x</sub>), sulfur oxides (SO<sub>x</sub>), ozone (O<sub>3</sub>), carbon dioxide (CO<sub>2</sub>) and particulate matter (PM<sub>2.5</sub>) (City of Toronto). Sources of emission include industrial processes, interior heating, vehicle traffic, dust, manufacturing, and construction (Bikis, 2023). Such emissions are linked to population density, as urban areas with greater human population condensed to a smaller area are prone to worsened air quality (Bikis, 2023). Another component of urban air pollution is vehicle road dust. Road dust can emerge through mechanical processing of metal, rock, and ore for industrial purposes (Khan & Strand, 2018). Such dust can become re-suspended on roads, dirt or paved, through the friction of tires (Figure 1). Road dust can contain metals, PM<sub>2.5</sub>, and other organic contaminants (Khan & Strand, 2018). Ultimately, urban air pollution, including gaseous pollutants and road dust, is a considerable threat to human health, as severe air pollution can cause health problems such as heart disease, stroke, lung cancer, and respiratory infections (Borck & Schrauth, 2021).

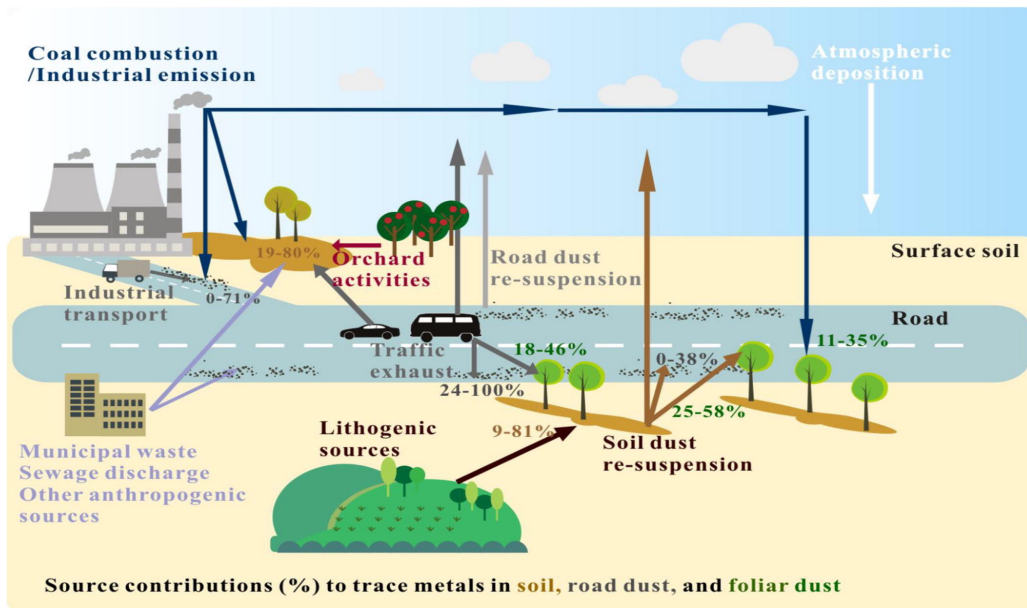


Figure 1. Road dust cycling in the environment. (Liang et. al., 2019).

As vehicles are one of the main sources of gaseous air pollutant emissions as well as road dust in the atmosphere, our study will consider the contribution of vehicle emissions of such pollutants. One place where vehicles are prevalent are drop-off zones in schools. Our study will collaborate with Toronto District School Board (TDSB) sustainability office to determine whether PM<sub>2.5</sub>, O<sub>3</sub>, and CO<sub>2</sub> emissions are higher during school drop-off times at Secord Public school compared to non drop-off times and weekends to evaluate whether or not walking or biking to school contributes to better air quality. Additionally, we will consider the concentrations of trace metals in road dust on streets with varying levels of vehicle traffic to evaluate the risk of metal inhalation from tire abrasion resuspending dust into the air where it can be inhaled. Gaseous air pollutants will be monitored using handheld monitors, and metals will be analyzed in road dust samples using Inductively Coupled Plasma Atomic Emission Spectroscopy (ICP-AES). By measuring both types of air pollutants, gaseous and road dust, a thorough risk assessment can be developed for the inhalation exposure of air pollutants from vehicle emissions.

### **Research Questions, Hypotheses, Goal, and Objectives**

*Overall Goal:* To inform students, teachers, and parents of the best school commute option that will not contribute to local urban air pollution.

*Research Question 1:* Are ambient concentrations of PM<sub>2.5</sub>, CO<sub>2</sub>, and O<sub>3</sub> higher during school drop-off times compared to non drop-off times?

*Research Question 2:* Does road dust from high-traffic areas contain a greater concentration of trace metals?

*Hypothesis 1:* Concentrations of PM<sub>2.5</sub>, CO<sub>2</sub>, and O<sub>3</sub> will be higher during school drop-off times compared to non drop-off times.

*Hypothesis 2:* Road dust collected from areas designated as high-traffic will contain greater concentrations of trace metal elements.

*Objective 1:* To effectively measure the ambient concentrations of gaseous air pollutants around Secord Public School at school drop-off times, during weekends and non drop-off times.

*Objective 2:* To effectively sample road dust using simple sampling techniques to identify and determine the concentration of elemental trace metals in the road dust.

## Materials and Methods

### Air Pollutant Monitoring

Essential air quality parameters, including CO<sub>2</sub>, O<sub>3</sub> and particulate matter smaller than 2.5 µm (PM<sub>2.5</sub>) were monitored at Secord Public School, an elementary school, in East York, Toronto, Ontario (Figure 2). The measurement occurred during the morning rush hours, corresponding to the period when students are being dropped off at the school, with the aim of examining the changes in air quality parameters during this timeframe. To comprehensively assess the air quality variations, the sampling timeframe was designated to be between 8:30 am and 9:30 am, coinciding with the period of when the majority of students are dropped off by parents, as the school's official commencement time is 9:00 am. To ensure a comprehensive analysis, data collection transpired during both weekdays and weekends, mitigating potential confounding factors associated with varying times of the day. The study sought to discern the specific impact of students arriving at the school by vehicle drop-off on air quality while minimizing the influence of temporal fluctuations inherent in different periods of the day.

The CO<sub>2</sub> and O<sub>3</sub> data were measured and recorded using AEROQUAL Series 500 Portable Air Quality Monitor and the PM<sub>2.5</sub> data was measured using HabitatMap AirBeam3 air quality sensor. The sensor, positioned at a height of 1.5 m above ground level, was strategically located in the drop-off zone for students. This placement aimed to simulate the average height of an elementary school student and capture air quality changes associated with vehicular emissions, including those from school buses.



**Figure 2.** Aerial image of Secord Public School. The black pin indicates where pollutant concentrations were measured during the sampling period. The image was taken from Ontario GeoHub.

The data was exported from the air quality sensors as .cvs files and cleaned manually to align the timestamps before being imported into R for data analysis and visualization. O<sub>3</sub> and PM<sub>2.5</sub> data at the same sampling time from the government air quality monitoring station nearby (Toronto East station) was also collected to serve as the background data for comparison.

### Road Dust

Six samples from locations with differing levels of traffic intensity were taken using plastic dust pans and sealed in polypropylene bags (Figure 3; Link A). Traffic levels were determined based on the City of Toronto road classification system where every street is given one of five classifications. Expressways were not considered due to safety concerns. All samples were collected on October 3, 2023 between 2:00 pm and 3:00 pm (Table A1). Plastic was used in these steps instead of metal to avoid potential contamination, as the analytes of interest are metals.

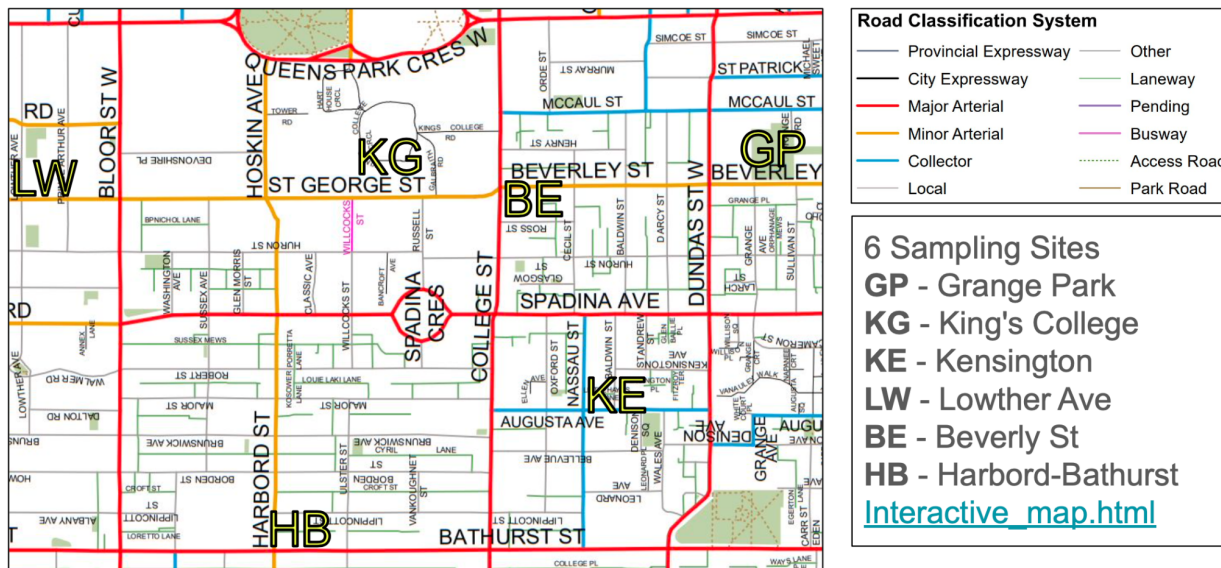


**Figure 3.** Map of road dust sampling sites. Top right legend indicates the road classification system based on Table A1. Bottom right legend indicates the sampling site code and full name of the site.

The samples were then taken to the laboratory and put through a 2.0 mm sieve in order to remove large particles, such as leaves and other organic matter. The sieve was blown with air between samples to avoid cross-contamination. Each sample was then ground with a mortar and pestle to achieve a fine powder, which provided more surface area for digestion. The samples were divided into three replicates for quality control (QC), and then each 0.5 g replicate was transferred to a microwave digestion tube along with 10 mL nitric acid. The replicates were then

microwaved for an hour. The acid and microwaving steps were performed in order to fully homogenize the dust matrix and to free the metals into solution. The replicates were then diluted with 100 mL DI water, and the extracts were filtered using a Whatman cellulose syringe filter, again in order to ensure that no particles of notable size were present in the analysis solution. Another 5 mL nitric acid was then added before making up a set of calibration standards using metal standards provided by the department. Finally, analysis was conducted for Na, Ca, Cu, Cr, Mg, Fe, Co, Cd, Pb, Zn, Mo, As, and Al via ICP-AES (Figure 4).

Data was exported as a .cvs from the ICP-AES instrument and plots and data analysis was conducted in Excel and R. R packages used for data cleaning and visualization includes: 'ggpmisc', 'dplyr', 'ggplot2', 'tidyverse', 'readxl', 'ggpmisc', 'tinytex', 'broom', 'ggh4x' and 'stringr'.

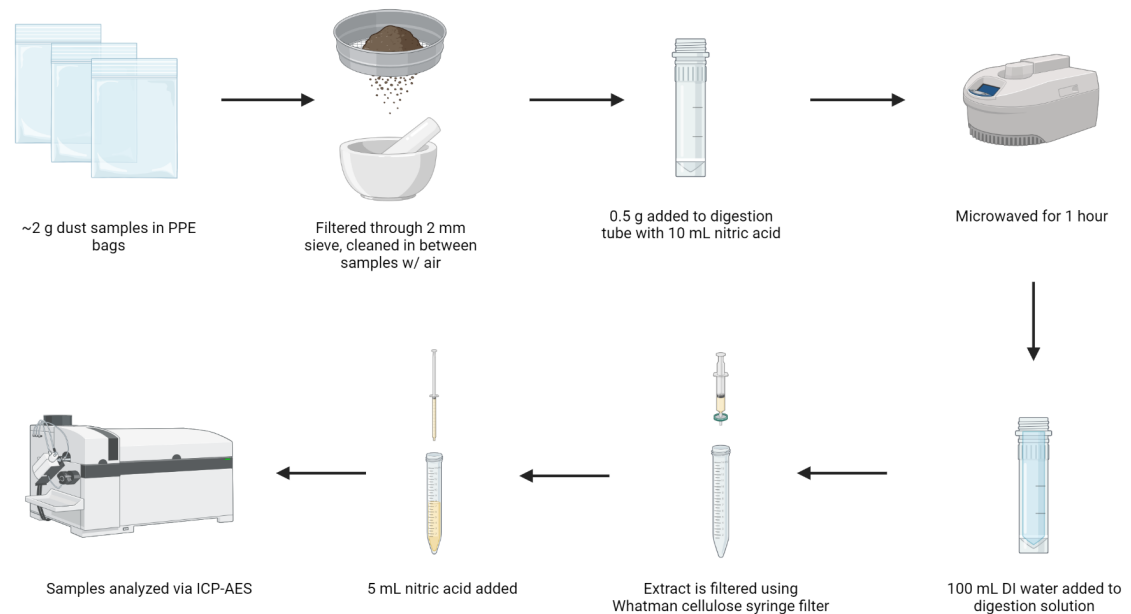


**Figure 4.** Road dust laboratory processing and analysis methods for elemental metal detection. Created with BioRender.com.

## Results and Discussion

### Air Pollutant Monitoring

CO<sub>2</sub>, O<sub>3</sub> and PM<sub>2.5</sub> monitoring data were measured and analyzed. Since the government air quality monitoring station does not collect CO<sub>2</sub> data, the CO<sub>2</sub> data was analyzed by comparing the weekday average against the weekend average.

There's an evident elevation in the CO<sub>2</sub> concentration on weekdays compared to the CO<sub>2</sub> level measured on weekends (Figure 5). This discrepancy suggests a direct correlation between heightened human and vehicular activities and the consequential increase in CO<sub>2</sub> concentration. Examining the weekend CO<sub>2</sub> data, the concentration of CO<sub>2</sub> experienced a surge before declining after around 9:10 am. This spike in concentration was likely attributed to morning human activities such as jogging, dog walking and commuting to work. These activities were observed to happen before 9:00 am. Subsequently, a notable decline in human activities is recorded after 9:00 am. When comparing these results to the background literature, one study found that CO<sub>2</sub> levels were higher during work zone congestion periods and lower during rush hour times (Zhang et al., 2011). Work zone congestion periods are designated as construction activity periods, which can indicate excess idling of vehicles, similar to school drop-off areas. In general, this temporal pattern lends support to the assertion that the elevated CO<sub>2</sub> concentration during weekdays is associated with the transportation of children to school.

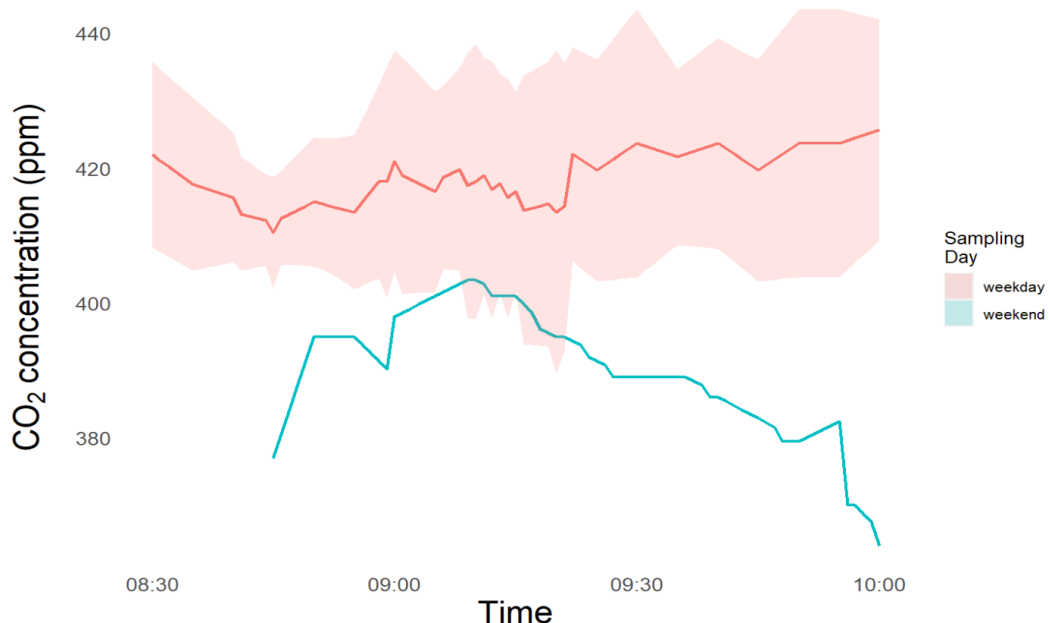


**Figure 5.** CO<sub>2</sub> concentration changes during and after morning drop-off hours on both weekdays and weekends. The solid line is the average CO<sub>2</sub> concentration and the shaded area is the average concentration ± standard deviation. Since only two weekend days' data is available, no standard deviation was calculated for weekend data.

The  $O_3$  data was compared to the government monitoring station nearby (Figure 6). The government monitoring station is located 6.4 km away from the sampling site near a major road. The selection of the government monitoring station as a reference site, due to its geographic proximity, allowed for the mitigation of potential confounding factors related to morning rush hour effects. Analysis of the data revealed a consistent pattern wherein the  $O_3$  concentration at the sampling site consistently exceeded that observed at the government monitoring location, irrespective of the day of the week. This discrepancy is attributed to the sampling site's closer proximity to the downtown area, characterized by heightened vehicular activities in comparison to the reference site. Notably, the  $O_3$  concentration during weekends is lower in comparison to the reference data, as opposed to the weekdays. This observation implies that vehicular activities near the school during drop-off times contribute to an increased local  $O_3$  concentration at the school. Background literature suggests that  $O_3$  concentrations can increase due to enhanced vehicle traffic, however other factors such as seasonality and sunlight exposure may have a greater impact on  $O_3$  concentrations (Mendoza et al., 2022). It is imperative to acknowledge the necessity for a more controlled comparative analysis to systematically eliminate potential extraneous factors and ensure the robustness of the conclusions drawn.

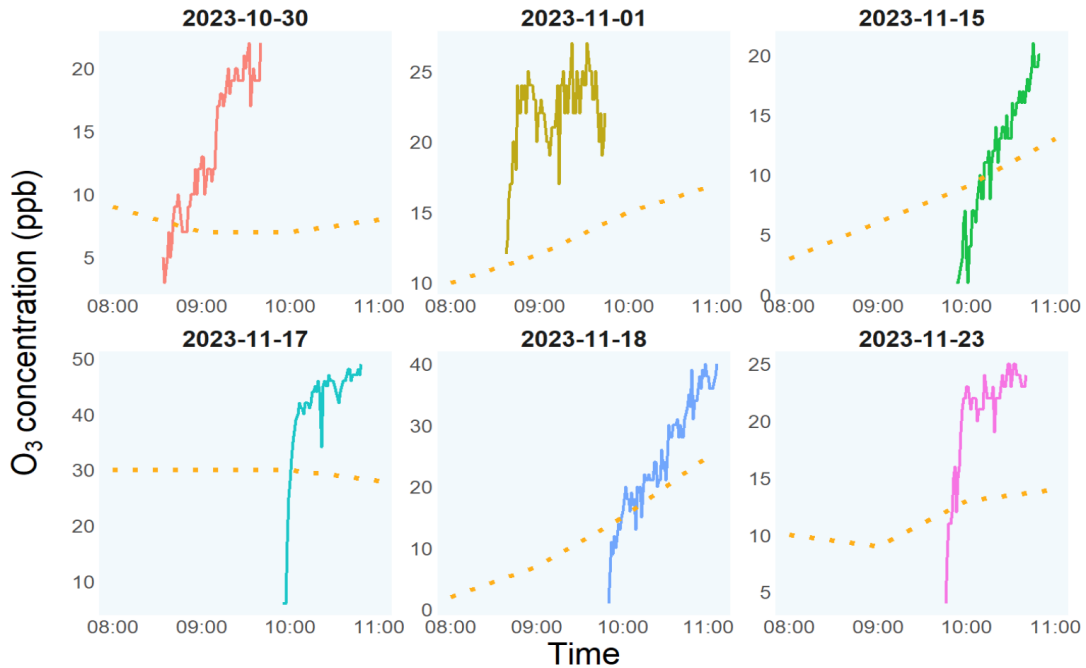


**Figure 6.** Ozone concentration (ppb) changes over time on the sampling days compared to data collected at the nearby government monitoring station. The solid line represents the  $O_3$  concentration at the sampling site while the orange dotted line shows the  $O_3$  concentration at the government monitoring station. The government monitoring data is hourly data. 2023-11-18 is the only weekend day  $O_3$  data is available and is shown in the plot in blue.

Similar to the  $O_3$  data analysis, the  $PM_{2.5}$  measurement was also compared against the  $PM_{2.5}$  measurement reference site. In contrast to the situation observed with  $O_3$ , the disparities between  $PM_{2.5}$  measurements taken at the sampling site and those at the reference site appear to exhibit a random distribution lacking a discernible pattern (Figure 7). This divergence is noteworthy, as it stands in contrast to the more structured discrepancies observed in the  $O_3$  data analysis. The unpredictability of the observed disparities in  $PM_{2.5}$  measurements is likely attributable to the multifaceted nature of factors influencing local  $PM_{2.5}$  concentrations. While local vehicular activities contribute to  $PM_{2.5}$  levels, the substantial impact of weather and broader regional human activities introduces additional complexities. Consequently, it is posited that the non-predictable nature of the observed  $PM_{2.5}$  measurement discrepancies may arise from the involvement of numerous variables in the dynamic changes of  $PM_{2.5}$  concentrations. In light of these findings, it is recommended that future studies adopt a more comprehensive approach to data collection, aiming to minimize the influence of extraneous variables and enhance the precision of the analysis.

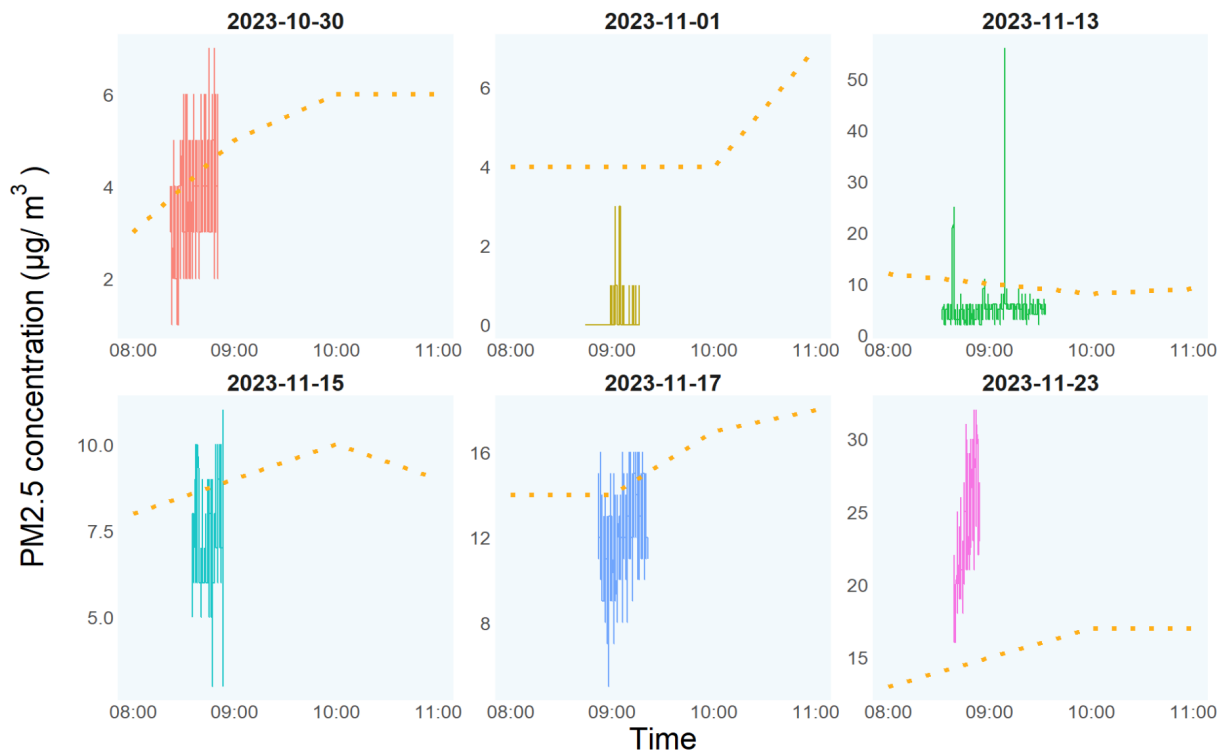
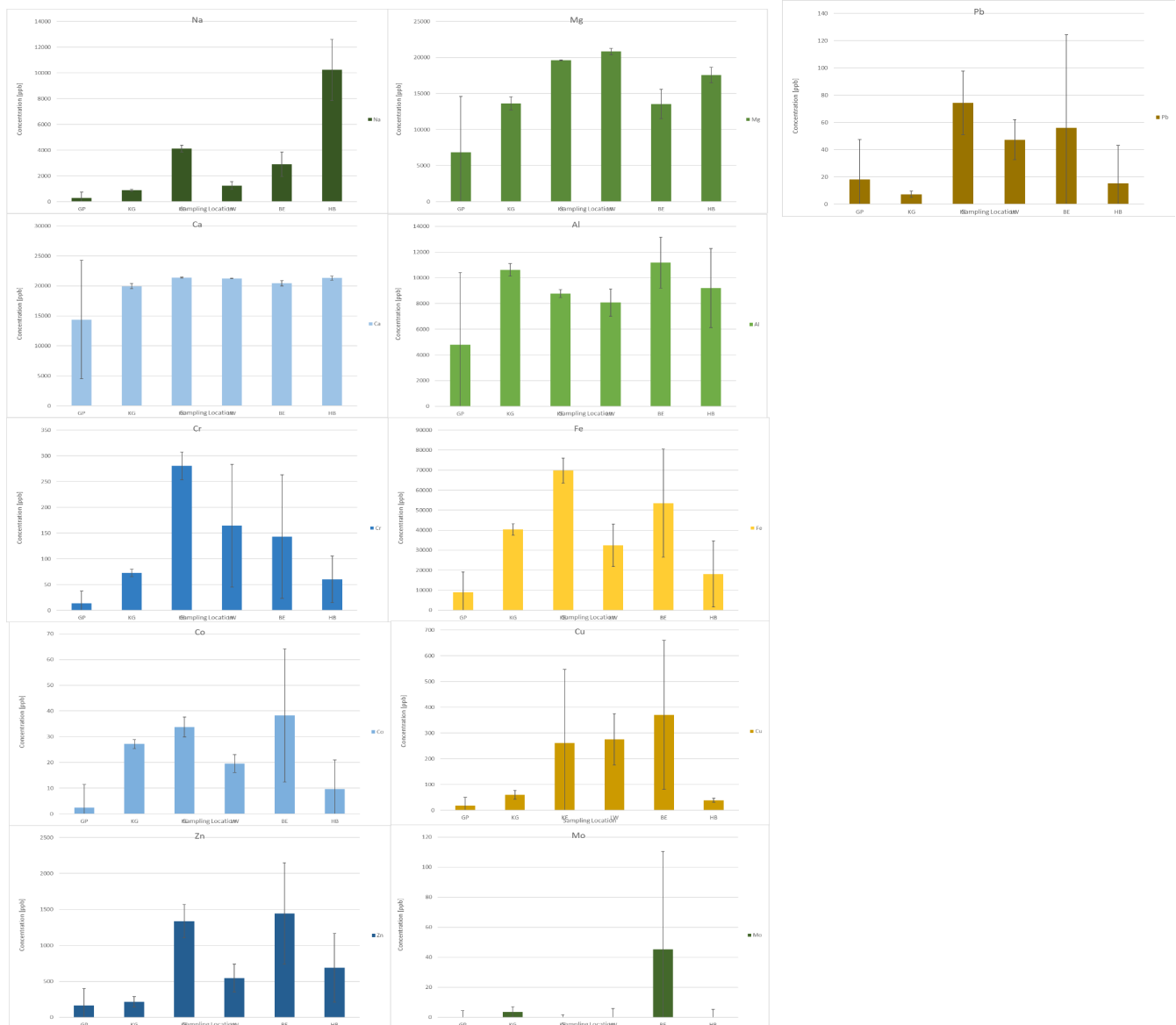


**Figure 7.**  $PM_{2.5}$  concentration ( $\mu\text{g}/\text{m}^3$ ) changes over time on the sampling days compared to data collected at the nearby government monitoring station. The solid line represents the  $PM_{2.5}$  concentration at the sampling site while the orange dotted line shows the  $PM_{2.5}$  concentration at the government monitoring station. The government monitoring data is hourly data.

## Road Dust

We aimed to quantify metal concentrations in road dust from areas of different traffic levels to determine if road dust from high-traffic zones contained higher concentrations of elemental trace metals using ICP-AES. The metals that are detected in the samples include Na, Ca, Cu, Cr, Mg, Fe, Co, Cd, Pb, Zn, Mo, As, and Al. A range of calibration curves (SI. Figure B1) were created from standards ranging from 1 ppb to 1000 ppb. Concentrations of each metal analyte were then calculated based upon their intensities (Figure 8). Concentrations of As and Cd have been reported as 0 (SI. Figure B2) as negative values were obtained, indicating concentrations likely below those in the blank and the LLOD.



**Figures 8:** Metal concentrations (ppb) in dust samples from varying traffic-level sites with standard deviation error bars. Traffic levels were determined with the Toronto Road Classification System (Table A1 of SI) increasing in anticipated vehicle volume from left to right.

Intensities of Al, Fe, Mg, Ca, and Na were well above those of the ULOQ from the highest standard concentration (1000 ppb) (Figure 8). This is likely due to the natural abundance of various metals. Previous studies have found that these metals can occur in large concentrations in road dust, specifically Al and Fe (Al-Taani et. al., 2019). Future studies should aim to dilute road dust samples by a factor of at least 100 to properly quantify concentrations of these metals if similar standards are to be used. Many metals are used in ion metabolism and transport such as Fe, Na, Ca, Mg, and Mo, which may explain their high concentrations from naturally decaying biological matter in road dust (Arnoud et. al., 2001).

Quantifiable metal concentrations above the LLOD and below the ULOQ included Mo, Zn, Pb, Co, Cr, and Cu. From this list, Cr and Pb are of considerable health concern due to their known toxicity (Baird & Cann, 2012). However, there are health and environmental concerns for the other metals observed in our road dust samples (Lee et. al. 2007; Lach et. al. 2018). Liang et. al. (2019) conducted a principal component analysis on road dust in Guangzhou and determined that Cu was a good indicator of overall car traffic contamination (Liang et. al., 2019). The concentrations for Cu in our samples ranged from  $18 \pm 31$  ppm in Grange Park to  $370 \pm 289$  ppm on Beverly Street. Contrary to the literature trend for copper, although Harbord-Bathurst is an intersection between major and minor arterial roads, it had very low Cu concentrations at  $38 \pm 8$  ppm. Regardless, a trend between Cu concentrations, as well as other metals, and traffic level persists which supports the scaling in traffic volume by the Toronto road classification system (Figure 9). However, the high variance between samples needs to be considered and further investigation on road-dust metal concentrations in relation to traffic in Toronto should be done.

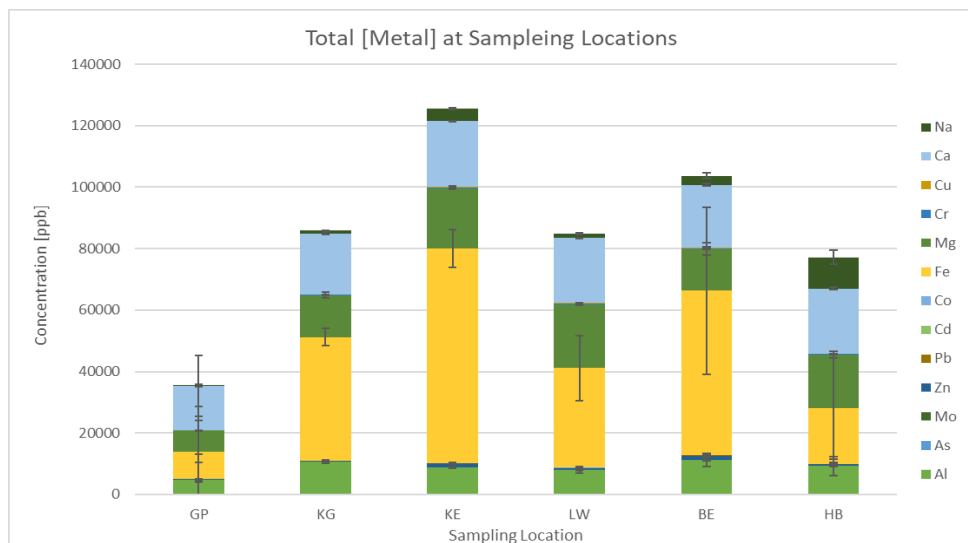


**Figure 9.** Concentration (ppb) of elemental trace metals detected at each sampling location, where codes are depicted in figure 3. Sampling locations are ordered from left to right in order of traffic level (low to high).

The percent recovery from the samples spiked with 0.5 mL of 1000 ppb standard is depicted in SI Table C1. Recovery of the samples was highly varied. No discernible trends were noticed between traffic level and recovery. Some interesting recoveries include recoveries from Al, Fe, Mg, Ca, and Na. Unsurprisingly, these were all analytes far beyond the ULOQ from the calibration standards.

### **Limitations and Recommendations to Future Students**

Our study had a few limitations due to factors out of our control. The overall goal of our project was to determine if vehicles were a significant source of gaseous air pollutants as well as metals in road dust nearby a school part of the TDSB. Although the air monitoring occurred at one of these schools, the road dust sampling occurred around the University of Toronto campus. Both of which are schools, but there are different land uses around each of the locations, thus creating inconsistency with matching our results together to relate them to school drop-off times. This limitation was due to the lack of equipment for both our group and another group to conduct gaseous air pollutant monitoring. Furthermore, the lack of equipment also carried over into the types of gaseous air pollutants we were able to monitor. NOx and SOx are some of the more toxic and prevalent air pollutants, and due to our equipment limitation, we were not able to measure these pollutants. Another limitation that we experienced is the lack of students driving into school at Secord Public School. By observation, there is a Toronto Transit Commission (TTC) stop nearby the school, and many students seem to walk since it is near a residential neighborhood. Students are also generally too young to bike to school, and therefore this sampling site could have been chosen better to represent an excess of vehicle emissions through pick-up and drop-off at another school that is not so close to the TTC and local neighborhoods. Finally, when sampling the road dust at locations with varying levels of traffic, it was difficult to estimate the amount of traffic at each location only given the road classification system. Therefore, our traffic estimations may not be fully accurate which has an impact on the reliability of our results.

Given our limitations, we recommend to future students planning sampling events far in advance, especially if you are required to share equipment with other groups and classmates. We also recommend using multiple sources to estimate traffic levels in Toronto, such as Google Maps in addition to the road classification system.

## **Conclusions and Future Work**

Both hypotheses are weakly supported, but due to the limitations and insignificance of the data, both hypotheses cannot fully be supported. For the air monitoring data, CO<sub>2</sub> and PM<sub>2.5</sub> levels were elevated over time and on weekdays, indicating contribution from vehicle drop-off emissions during the sampling time. For road dust, low traffic areas had lower concentrations of metals and high traffic areas had, on average, higher concentrations of metals, but there was not a significant difference between concentrations.

The continuation of this project could examine larger sample sizes of measurements of CO<sub>2</sub>, O<sub>3</sub> and PM<sub>2.5</sub> on weekends to improve the significance of the results. Future research could examine air pollutants such as SO<sub>2</sub> and NO<sub>x</sub> for a more comprehensive view of the air quality at the school site. The study could also be replicated at other schools, while considering the major mode of transportation at such schools. We could also explore a correlation between pollutants and meteorological conditions, considering temperature, wind speed and humidity, as they have been shown to impact the levels of O<sub>3</sub>, NO<sub>x</sub> and PM<sub>10</sub> in the atmosphere (Perez, 2021). In addition, we could consider conducting a prolonged study to observe seasonal trends over time. Lastly, we can organize community workshops to raise awareness about air quality and discuss the related health implications from the choice of the mode of commute.

## References

1. Al-Taani, A. A., Nazzal, Y., & Howari, F. M. (2019). Assessment of heavy metals in roadside dust along the Abu Dhabi-Al Ain National Highway, UAE. *Environmental Earth Sciences*, 78(14), 1–13. <https://doi.org/10.1007/s12665-019-8406-x>
2. Atmosphere | Free Full-Text | Air Quality and Behavioral Impacts of Anti-Idling Campaigns in School Drop-Off Zones. <https://www.mdpi.com/2073-4433/13/5/706> (accessed 2023-12-08).
3. Baird, C. and Cann, N. (2012) Environmental Chemistry. 5th Edition, W. H. Freeman and Company, New York.
4. Bikis, A. Urban Air Pollution and Greenness in Relation to Public Health. *Journal of Environmental and Public Health* **2023**, 2023, e8516622.
5. Borck, R.; Schrauth, P. Population Density and Urban Air Quality. *Regional Science and Urban Economics* **2021**, 86, 103596. <https://doi.org/10.1016/j.regsciurbeco.2020.103596>. <https://doi.org/10.1155/2023/851662>
6. Khan, R. K.; Strand, M. A. Road Dust and Its Effect on Human Health: A Literature Review. *Epidemiol Health* **2018**, 40, e2018013. <https://doi.org/10.4178/epih.e2018013>.
7. Lach, K.; Bernatíková, Š.; Frišhansová, L.; Klouda, K.; Mička, V. STUDY OF AIR CONTAMINATION BY HEAVY METALS AT FIRING RANGES; Naples, Italy, 2018; pp 29–39. <https://doi.org/10.2495/AIR180031>.
8. Lee, C. S. L.; Li, X.-D.; Zhang, G.; Li, J.; Ding, A.-J.; Wang, T. Heavy Metals and Pb Isotopic Composition of Aerosols in Urban and Suburban Areas of Hong Kong and Guangzhou, South China—Evidence of the Long-Range Transport of Air Contaminants. *Atmospheric Environment* **2007**, 41 (2), 432–447. <https://doi.org/10.1016/j.atmosenv.2006.07.035>.
9. Liang, S.-Y.; Cui, J.-L.; Bi, X.-Y.; Luo, X.-S.; Li, X.-D. Deciphering Source Contributions of Trace Metal Contamination in Urban Soil, Road Dust, and Foliar Dust of Guangzhou, Southern China. *Science of The Total Environment* **2019**, 695, 133596. <https://doi.org/10.1016/j.scitotenv.2019.133596>.
10. Pérez, I. A., García, M. Á., Pérez, I. A., & García, M. Á. (2021). *Air Pollution Meteorology*. MDPI - Multidisciplinary Digital Publishing Institute.
11. Toronto, C. of. *Air Pollution*. City of Toronto. <https://www.toronto.ca/community-people/health-wellness-care/health-programs-advice/air-quality/air-pollution-and-health/> (accessed 2023-12-08).

12. Toronto, C. of. *Road Classification Maps*. City of Toronto.  
<https://www.toronto.ca/services-payments/streets-parking-transportation/traffic-management/road-classification-system/maps-and-indices/> (accessed 2023-12-08).
13. van Vliet, A. H. M.; Bereswill, S.; Kusters, J. G. Ion Metabolism and Transport. In *Helicobacter pylori: Physiology and Genetics*; ASM Press: Washington (DC), 2001.
14. Zhang, K.; Batterman, S.; Dion, F. Vehicle Emissions in Congestion: Comparison of Work Zone, Rush Hour and Free-Flow Conditions. *Atmospheric Environment* **2011**, *45* (11), 1929–1939. <https://doi.org/10.1016/j.atmosenv.2011.01.030>.

## **Supplemental Information**

### **A. Road Dust Sample Collection Sites**

**Table A1.** The Road classification system used by the City of Toronto based on traffic volumes and the road class of each road dust sampling location

Road Class	Criteria
Local (GP, KC, LW)	Less than 2,500 vehicles per day Low traffic speed Generally no bus routes Cyclists – special facilities as required Sidewalks on at least one side of road Truck restrictions preferred Low priority for winter maintenance
Collector (KS)	2,500 to 8,000 vehicles per day Less than 1,500 bus (or streetcar) passenger per day Signalized intersections at arterial roads Truck restrictions permitted Cyclists – special facilities as required Sidewalks on both sides of the road Medium priority for winter maintenance
Minor Arterial (BE)	8,000 to 20,000 vehicles per day 1,500 to 5,000 bus passenger per day Speed limits 40 to 60 km/h No “Stop” signs; main intersections controlled by traffic signals No truck restrictions Sidewalks on both sides High priority of winter maintenance
Major Arterial (HB)	Greater than 20,000 vehicles per day Greater than 5,000 bus passengers per day Speed limits 50 to 60 km/h Cyclists – special facilities desirable Sidewalks on both sides High priority of winter maintenance
Expressway	Speed limits 80 to 100 km/h Greater than 40,000 vehicles per day No local transit service Pedestrians and cyclists prohibited Grade-separated intersections (no traffic signals) Highest priority of winter maintenance



**Figure A1.** The preview image of an interactive map showing the location and traffic intensity at each sampling site. An interactive map showing the location and traffic intensity at each sampling site. The full interactive map can be accessed at

<https://drive.google.com/uc?id=1IItv-U4b26X6YsK9fLq3jfNuI1BbGQlZ>

## B. Calibration curves used in ICP analysis

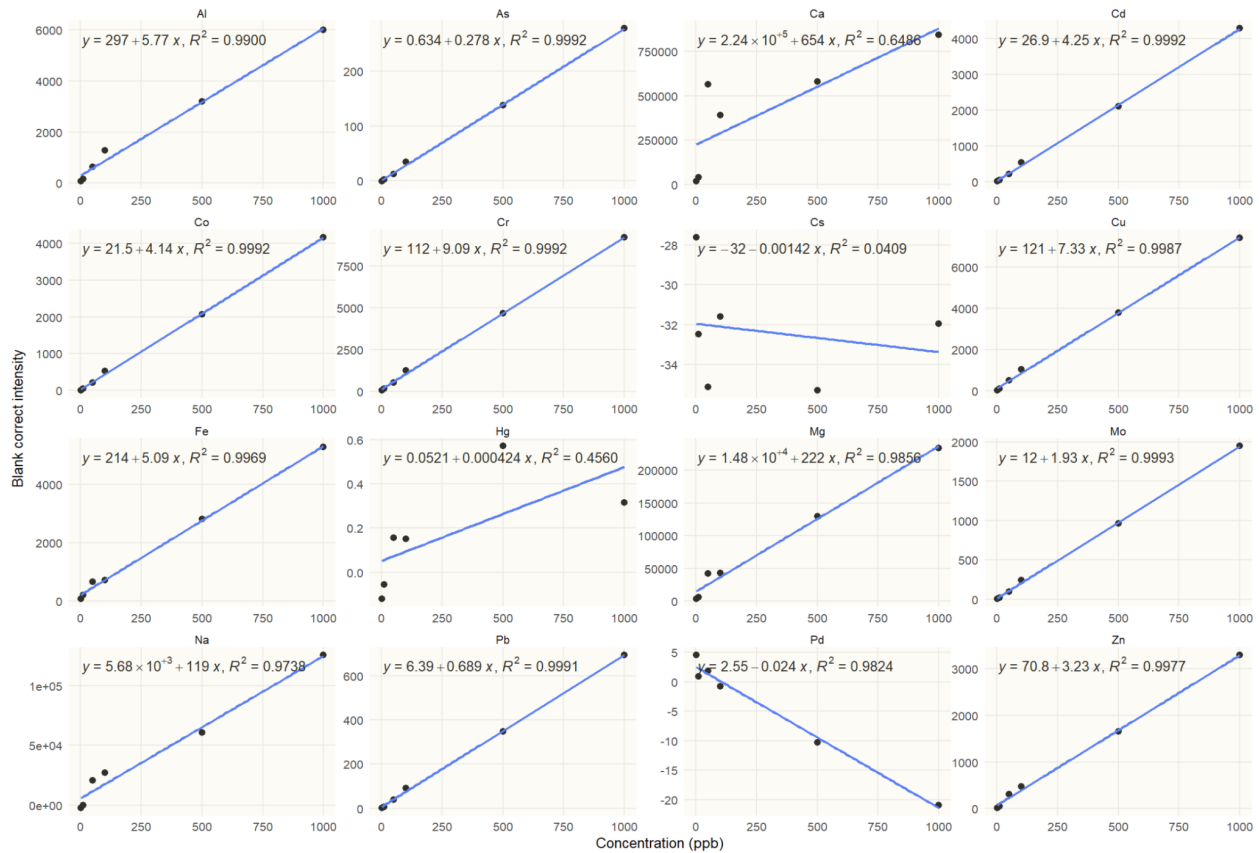


**Figure B1.** The calibration curve used for ICP analysis. The calibration curves show the linear correlations between sample concentration (ppb) and measured intensity for each element. The linear regression equation and their coefficients of determination are also shown in the figure.

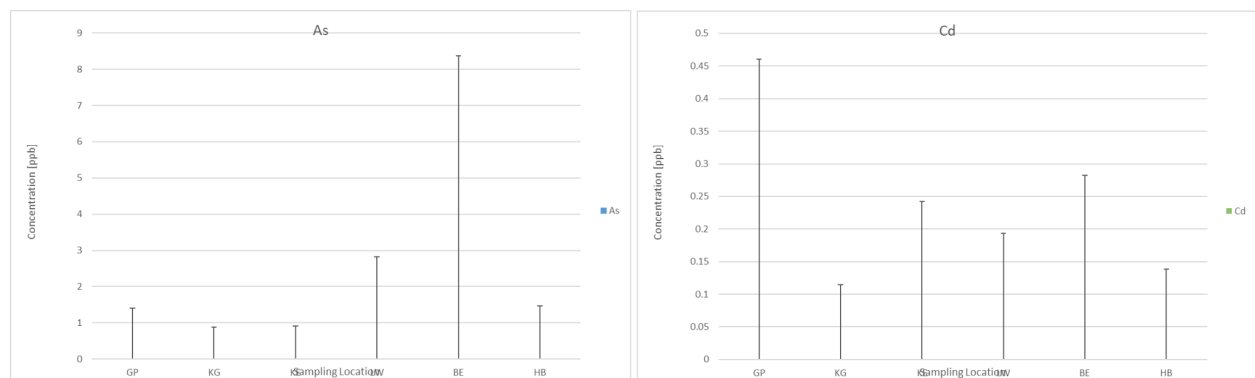


**Figure B2.** Unquantifiable negative readings from Arsenic and Cadmium.

## C. Road Dust Samples Results

**Table C1.** Element recovery rate of all road dust samples.

Site	Element Recovery (%)												
	Al	As	Mo	Zn	Pb	Cd	Co	Fe	Mg	Cr	Cu	Ca	Na
GP	79	18	16	32	17	17	16	633	237	18	18	-104	50
HB	89	17	17	71	21	17	19	3966	298	30	23	-116	1170
KC	-266	19	17	14	16	18	16	-898	-255	15	16	-168	-8
KE	234	17	16	135	23	17	19	5509	84	40	28	-120	357
BE	-34	18	24	120	19	18	24	7108	555	38	49	44	386
LW	257	18	18	90	19	17	16	1947	-11	61	28	-53	60

**Table C2.** Blank-corrected element concentration (ppb) calculated using the calibration curve.

Site	Element concentration (ppb)												
	Al	As	Mo	Zn	Pb	Cd	Co	Fe	Mg	Cr	Cu	Ca	Na
GP	4784	<LOD	<LOD	165	18.12	<LOD	2.377	9018	6830	13.66	18.33	14388	287.1
KG	10615	<LOD	3.622	216.5	7.3	<LOD	27.13	40364	13632	72.54	59.1	19952	882.6
KE	8763	<LOD	<LOD	1336	74.3	<LOD	33.79	69770	19611	280.36	260.43	21390	4126
LW	8067	<LOD	0.1673	546.4	47.27	<LOD	19.57	32423	20826	164.37	274.7	21241	1248
BE	11182	<LOD	45.14	1444	55.9	<LOD	38.27	53496	13542	143.15	370.5	20442	2902
HB	9206	<LOD	<LOD	689.7	15.26	<LOD	9.639	18094	17557	60.16	38.73	21314	10232

**Table C3.** The standard deviation of blank corrected element concentration calculated using the calibration curve.

Site	Standard deviation (ppb)												
	Al	As	Mo	Zn	Pb	Cd	Co	Fe	Mg	Cr	Cu	Ca	Na
GP	5605	1.403	4.425	233.3	29.32	0.4607	9.044	10051	7764	24.05	31.80	9898	454.9
KG	488	0.888	3.429	73.34	2.326	0.1144	1.773	2816	916.9	7.150	16.64	438.1	80.50
KE	314	0.914	1.786	229.6	23.29	0.2422	3.878	6168	26.86	26.89	286.6	83.60	267.7
LW	1059	2.827	5.688	192.3	14.59	0.1937	3.486	10621	442.3	119.1	100.1	9.222	306.7
BE	1987	8.370	65.25	702.6	68.36	0.2826	25.84	27089	2027	119.8	289.5	435.0	957.7
HB	3074	1.471	5.231	476.7	27.85	0.1389	11.33	16472	1069	45.19	8.23	333.7	2369